Fuel 112 (2013) 74–82

Contents lists available at SciVerse ScienceDirect

Fuel

journal homepage: www.elsevier.com/locate/fuel

Co-pyrolysis of low rank coals and biomass: Product distributions

Ryan M. Soncini [a,b], Nicholas C. Means [a,b], Nathan T. Weiland [a,c,*]

[a] National Energy Technology Laboratory, Pittsburgh, PA, United States
[b] URS Corporation, Pittsburgh, PA, United States
[c] Mechanical & Aerospace Engineering Dept., West Virginia Univ., Morgantown, WV, United States

HIGHLIGHTS

- Co-pyrolysis of pine wood with lignite and sub-bituminous coal is studied.
- Isothermal semi-batch tests increase particle contact and reduce secondary reactions.
- Non-additive synergy in tar production is observed.
- Evidence of rapid hydrogen evolution from biomass stabilizing coal tar radicals.
- Eight product distributions curve fit to temperature and blend ratio for modeling.

ARTICLE INFO

Article history:
Received 23 January 2013
Received in revised form 19 April 2013
Accepted 24 April 2013
Available online 17 May 2013

Keywords:
Coal
Biomass
Co-pyrolysis
Low rank coal

ABSTRACT

Pyrolysis and gasification of combined low rank coal and biomass feeds are the subject of much study in an effort to mitigate the production of green house gases from integrated gasification combined cycle (IGCC) systems. While co-feeding has the potential to reduce the net carbon footprint of commercial gasification operations, success of this strategy requires investigation of the effects of coal/biomass co-feeding on reaction kinetics and product distributions. Southern yellow pine was pyrolyzed in a semi-batch type drop tube reactor with either Powder River Basin sub-bituminous coal or Mississippi lignite at several temperatures and feed ratios. Product gas composition of expected primary constituents (CO, CO_2, CH_4, H_2, H_2O, and C_2H_4) was determined by in situ mass spectrometry while minor gaseous constituents were determined using a GC–MS. Product distributions are fit to linear functions of temperature, and quadratic functions of biomass fraction, for use in computational co-pyrolysis simulations.

The results are shown to yield significant nonlinearities, particularly at higher temperatures and for lower ranked coals. The co-pyrolysis product distributions evolve more tar, and less char, CH_4, and C_2H_4, than an additive pyrolysis process would suggest. For lignite co-pyrolysis, CO and H_2 production are also reduced. The data suggests that rapid pyrolysis of biomass produces hydrogen that stabilizes large radical structures generated during the early stages of coal pyrolysis. Stabilization causes these structures to be released as tar, rather than crosslinking with one another to produce secondary char and light gases. Finally, it is shown that, for the two coal types tested, co-pyrolysis synergies are more significant as coal rank decreases, likely because the initial structure in these coals contains larger pores and smaller clusters of aromatic structures which are more readily retained as tar in rapid co-pyrolysis.

1. Introduction

Coal is an abundant natural resource in the United States with more than 1.6 trillion short tons remaining, enough to meet current domestic demand for 1600 years [1,2]. A primary concern with coal utilization is the release of carbon dioxide, the second greatest contributor to the green house effect [3]. The addition of biomass to a coal conversion process reduces the carbon footprint of that process because, from an atmospheric perspective, biomass thermal conversion is inherently carbon neutral. This carbon neutrality stems from the various carbon fixation pathways plants use to grow, synthesizing carbohydrates from atmospheric carbon dioxide [4]. Furthermore, much of the carbon contained in biomass is fated to return to the atmosphere if left unutilized as the natural decay of organic materials results in the release of carbon dioxide and methane gases [5]. The renewable nature and high availability of biomass are likely why it is the third most utilized energy source in the world behind oil and coal [6,7]. Woody biomass is of particular interest as forest harvesting and wood processing residues have potential for significant energy production.

* Corresponding author at: Mechanical & Aerospace Engineering Dept., West Virginia Univ., Morgantown, WV, United States.
E-mail addresses: nathan.weiland@mail.wvu.edu, nathan.weiland@netl.doe.gov (N.T. Weiland).

0016-2361/$ - see front matter © 2013 Elsevier Ltd. All rights reserved.
http://dx.doi.org/10.1016/j.fuel.2013.04.073

Thermochemical conversion of carbonaceous materials such as coal and biomass is a complex process that involves numerous homogeneous and heterogeneous reactions. Conversion begins with the pyrolysis or devolatilization reaction, a thermal decomposition process resulting in the release of various gases and tar from the feed while leaving a high carbon char. Pyrolysis of biomass evolves gases more rapidly than coal due to the relatively lower bond energies of ether (R—O—R) and C—C bonds associated with lignocellulosic biomass, compared to the C=C aromatic bonds typically found in the molecular structure of coal [8]. The primary focus of this work is the study of pyrolysis as a precursor to gasification. In most commercial gasification operations pyrolysis takes place separately from char conversion reactions, warranting the in-depth study of the devolatilization process [9].

Reports of non-linear, synergistic effects on kinetics and product distributions in previous studies of coal/biomass co-pyrolysis vary, depending on heating rate, temperature, and proximity of coal and biomass particles to one another. Many co-pyrolysis studies have been performed using thermogravimetric analysis (TGA) [10–15]. These experiments typically do not show non-linear effects, in part because biomass and coal volatiles evolve at different times due to relatively slow heating rates [12,13]. In fact, synergies have only been noted for very low rank lignite and peat, where coal and biomass volatile evolution regimes overlap [11].

High heating rate experiments are more representative of actual conditions in most types of gasifiers, though the results from such studies are mixed with respect to synergy in co-pyrolysis. In these studies, the proximity of coal and biomass particles to one another during co-pyrolysis plays a significant role, where the volatile cloud surrounding a biomass particle should be in contact with a coal particle for any interactions to occur. As a result, co-pyrolysis synergies are either found to be non-existent [8,16] or fairly slight [17,19] in a traditional drop-tube reactor, depending on particle sizes and feed rates. Where close coal/biomass particle contact is maintained in the reactor, synergies are often found to be significant [19–21]. In coal pyrolysis, radical volatiles released during the initial pyrolysis stages engage in gas-char reactions that promote recombination and crosslinking within the char [22–25]. This process impedes the later adsorption of gasification agents to carbon active sites, thus reducing char reactivity of pure coal feed [22,23]. Biomass co-feeding at high heating rates and close particle contact may prevent this recombination phenomenon by stabilizing free radicals through atomic hydrogen donation [18,26]. As a result, some high heating rate studies have shown that coal char reactivity is improved when co-pyrolyzed with biomass [17–19,26].

One gasifier type where high heating rates and frequent particle interactions are prevalent is the transport, or circulating fluidized bed, gasifier, which has been identified as an effective platform for gasification of low rank fuels [27,28]. A pilot scale transport gasifier has been in operation at the Univ. of North Dakota for many years, and the demonstration scale Transport Integrated Gasifier (TRIG™) has operated at the National Carbon Capture Center (NCCC) in Wilsonville, AL since 1999. A 582 MW commercial scale IGCC unit under construction in Kemper County, Mississippi, is currently slated for startup in 2014.

Development of transport gasifier technology can be greatly accelerated with the aid of multi-phase computational modeling tools. While such models exist, and have been used to study the TRIG and other transport gasifiers [29–31], they currently lack the kinetics and product distribution data required to properly model the non-linear interactions that may occur with coal/biomass co-feeding. The current work is part of a larger effort to provide co-pyrolysis and co-gasification data for feedstocks and operating conditions of interest to transport gasification applications. Several coal/biomass co-feeds tests have already been run in the TRIG, providing the opportunity to validate kinetics and multi-phase modeling of co-feed transport gasification [28]. To this end, the present work employs the same feedstocks used in the TRIG at NCCC, and the resulting kinetics and product distributions for co-pyrolysis and co-gasification testing will be fed into NETL's Carbonaceous Chemistry for Computational Modeling (C3M) software platform, which is a kinetics clearinghouse and analysis tool for use with high-fidelity, multi-phase CFD packages [32]. Although the data generated under this program finds its primary application with modeling the TRIG reactor and its progeny, it can be used for modeling other conversion processes through the C3M program, which delivers the first commercially available coal/biomass co-feed kinetic database.

2. Experimental details

2.1. Feedstocks

All feeds were acquired from the Power Systems Development Facility (PSDF), a pilot scale transport gasifier operated by the Southern Company that researches semi-commercial scale power systems components as part of the NCCC. The low rank coals used in this study were a sub-bituminous B coal from Wyoming's Powder River Basin (PRB) and a Mississippi lignite (LIG) mined from Red Hills Mine in Ackerman, Mississippi, which were received in a pulverized form. The woody biomass (WB) feedstock used is southern yellow pine, supplied to PSDF in pelletized form by Green Circle BioEnergy. The biomass pellets were reground and all feeds were separately sieved into various particle regimes. The size feeds used in this study were 106–300 μm. Feeds were dried at 105 °C for approximately 24 h and stored in a desiccator. Feed ratios used in this study are presented in Table 1.

Proximate and ultimate analyses of the coals and biomass were conducted by Consol Energy. The results from these analyses are presented in Table 2. Several potential benefits of these feeds may be seen from the proximate and ultimate analyses. It can be seen that the H:C mass ratio for the coals is relatively low compared to that of the biomass. Many chemical operations require hydrogen rich synthesis gas for optimum production of desired product. The higher H:C mass ratio of WB suggests that biomass may act as a hydrogen donor to the gasification process and reduce the need for H_2:CO conditioning techniques such as recycle and water–gas shift. Lastly, the low sulfur contents for all feeds are beneficial as acid gas removal costs can be limited by reducing the amount of gaseous sulfur seen by the system.

2.2. Experimental setup and procedure

Product distribution testing was performed by pyrolyzing approximately 0.1 g of 106–300 μm feed at 600, 700, 800, 900, and 975 °C. A schematic of the reactor configuration used for these experiments is shown in Fig. 1. Details concerning the general construction of the reactor can be found elsewhere [34]. The quartz frit for this study is located 15 in. from the top of an 18 in. heating zone. A specialized quartz reactor liner was designed to reduce

Table 1
Feed ratios (wt%).

PRB/WB	LIG/WB
100/0	100/0
90/10	–
80/20	80/20
50/50	50/50
0/100	0/100

Table 2
Proximate and ultimate analyses.

Sample	PRB	LIG	WB
Proximate Analysis (wt%, dry basis)			
Volatile	46.18	43.76	85.10
Ash	6.60	25.71	0.64
Fixed Carbon	47.22	30.53	14.26
Ultimate Analysis (wt%, dry basis)			
Carbon	66.21	51.75	48.84
Hydrogen	4.20	3.57	5.78
Nitrogen	1.21	1.27	0.38
Oxygen (diff)	21.30	16.97	44.21
Sulfur	0.48	0.73	0.15

the residence time of product gases in an effort to minimize the occurrence secondary pyrolytic reactions. The nozzle was lightly packed with quartz wool to capture any char that may have gone around the frit.

Experiments were conducted using an argon sweep gas flow rate of 4.5 slpm under atmospheric pressure. When the reactor reached thermal equilibrium, the sample was dropped into the reactor where it contacted the hot quartz frit, pyrolyzing the sample. Calculated sample drop times range from 0.6 to 1.6 s, depending on particle size and reactor temperature, and some particle heating may occur during this time. High speed optical pyrometer measurements of the top of the frit were performed for a few test cases, and show that most of the particle heating occurs on contact with the frit, at heating rates ranging from 400 to 1000 K/s. Gaseous and liquid products are rapidly removed from the reactor by the sweep gas and sampled by a mass spectrometer. Assuming plug flow conditions, the total residence time of volatile pyrolysis products in the reactor is approximately 0.15 s, effectively minimizing tar cracking and secondary pyrolysis reactions. Product gas is sampled at a rate of 1.4 Hz by a Pfeiffer OmniStar quadrupole mass spectrometer (QMS) to evaluate concentrations of H_2, CH_4, H_2O, C_2H_4, CO, H_2S, Ar, and CO_2. The calibration of the QMS is checked prior to every experiment with a NIST-traceable gas mixture containing approximately 50% Ar, 25% CO, 5% CO_2, 10% CH_4, and 10% H_2, and this data is used to correct the recorded experimental data for drift in the QMS calibration. This data is then integrated over the complete reaction to yield the total gas species evolved. Attempts were also made to quantify H_2S product gas, but quantities were too small to be measured by mass spectrometry for these low sulfur fuels. As a check, an oxygen balance is calculated between the reactants and gas products, and gas data from test runs with excessive oxygen balances (>120%) are excluded in the final results. The gas tubing between the reactor and QMS sample site is maintained at 150 °C or higher to prevent volatiles from condensing and clogging the QMS transfer line. Products are then carried through a copper coil and quartz wool filter, all submerged in an ice bath, to remove the remaining condensable products from the effluent stream before being vented.

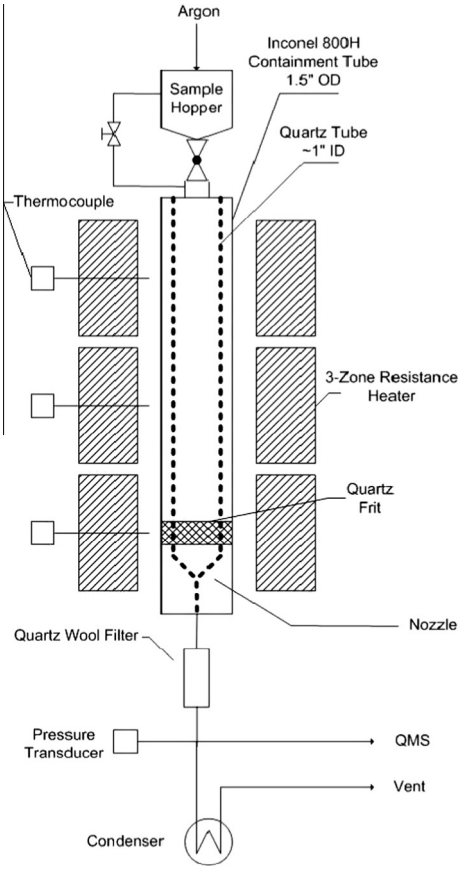

Fig. 1. Schematic of semi-batch drop tube reactor.

A few additional experiments were conducted to generate gas and tar samples for analysis of minor constituents. These experiments were conducted by pyrolyzing 1 g of the 500–850 μm feed at 600 °C, 800 °C, and 975 °C. The reactor configuration used is very similar to that in Fig. 1, except that additional filters are added to capture tars. Also, a portion of the product gas is collected in a gas bag after the condenser and filters for GC–MS analysis in a PerkinElmer Clarus 500.

For the purposes of utilizing the product distribution results of this study in C3M or other computational programs that model co-pyrolysis processes, a multivariate regression analysis is used to determine best-fit parameters to the following general equation for the mass fraction, Y_i, of product i, given as a weight fraction of the original dried feedstock weight:

$$Y_i = a_0 + a_X X + a_{XX} X^2 + a_T T + a_{XT} XT + a_{XXT} X^2 T \quad (1)$$

where X is the biomass weight fraction and T is the pyrolysis temperature in units of °C. Once the coefficients of Eq. (1) for char, CO, CO_2, H_2, H_2O, CH_4 and C_2H_4 are determined, then similar coefficients for tar can be computed by difference from:

$$Y_{tar} = 1 - \sum_i Y_i \quad (2)$$

Calculation of the tar in this manner enforces conservation of mass in the pyrolysis process when using the curve fits to determine product distributions.

3. Results and discussion

3.1. Overall product distributions

Gas, char, and water product isotherms for PRB/WB and LIG/WB at 600 °C and 975 °C are presented in Fig. 2. On the whole, it can be seen that gas and water increase with increasing biomass wt% while the amount of char remaining declines. Increase in gas evolution with biomass wt% is expected due to the large volatile content of the biomass. Mixtures of PRB/WB and LIG/WB present similar major product distributions as a function of biomass weight percent. This is expected, given the similar volatile, char, and ash contents of the two coal feedstocks, as seen in the proximate analysis of Table 2. In general, lignite and its blends produce more gas and water, and less char, than PRB coal blends at low temperature, with the opposite trend at higher temperatures.

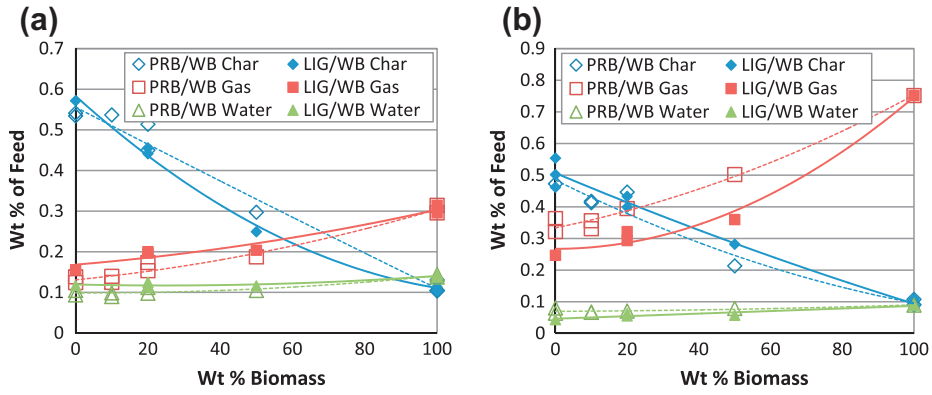

Fig. 2. Product distributions for (a) 600 °C and (b) 975 °C.

Another trend that is evident in Fig. 2 is the relative linearity in the PRB/WB product distributions, and the non-linearity in LIG/WB products, particularly for char production at low temperature and gas production at high temperature. This nonlinearity is consistent with the observations of Haykiri-Acma and Yaman [11], who note that lower rank coals are more susceptible to nonlinear interactions when co-pyrolyzed with biomass.

Figs. 3 and 4 show the changes in char, gas and tar production over the temperature and feedstock blend space tested in this study. Data points are shown as circles, while the mesh represents the curve fits from Eq. (1). For both feedstock blends in Figs. 3 and 4, linearity with respect to temperature is readily apparent, and agrees with the results of similar wood/coal [18,20] and other lignocellulosic biomass/coal co-pyrolysis studies [17,19]. The gas and char trends for the PRB/WB mixture in Fig. 3 are relatively linear in biomass wt%, with slight nonlinearities. A slight nonlinearity also appears in the water production (see Fig. 5d), which is not included in the gas fractions, such that computation of the tar by difference in Fig. 3c yields a more significant non-linearity in biomass fraction, particularly at higher temperatures.

LIG/WB char product fractions in Fig. 4a are roughly linear with respect to temperature and biomass feed fraction at high temperature, though biomass fraction nonlinearities appear at lower temperatures. Gas product fractions in Fig. 4b appear to be nonlinear with respect to biomass fraction at temperatures above 700 °C. The resulting LIG/WB tar production in Fig. 4c is very nonlinear, indicating more significant co-pyrolysis synergies than for PRB/WB fuel mixtures.

Quantitative agreement with literature is difficult to assess due to variances in gas and liquid collection and reporting methods, however, char data was compared to data or regression coefficients of similar studies, and showed strong quantitative agreement [16,18,20]. Qualitatively, the trends in Figs. 3 and 4 are consistent with similar studies of pine biomass/coal co-pyrolysis. In particular, isothermal drop-tube experiments performed by Zhang and colleagues show slight, though similar, nonlinearities with respect to biomass weight fraction for bituminous and brown coals, though their experiments were only performed up to 700 °C [17,18]. Fixed bed co-pyrolysis experiments with sawdust and sub-bituminous coal are shown to yield nonlinearities in product yields at lower temperatures (500–700 °C), with more linear distributions with respect to biomass fraction and temperature at 800 °C [20]. However, the fixed bed arrangement in Park's experiment allows sufficient bed residence time for tar cracking reactions to occur, yielding high gas fractions and low tar fractions relative to additive co-pyrolysis behavior [20]. Further, the experiments of Yuan and colleagues are very similar to those of this study, although tar residence times are roughly an order of magnitude higher than in the present study. Yuan et al.'s study yields similar results to this work at low temperatures, while at higher temperatures, synergistic gas products are favored over tar products, a result which is attributed to increased tar cracking [19].

Since tar cracking residence times are actively minimized in the current experimental configuration, Figs. 3 and 4 show that synergies in low rank coal/biomass co-pyrolysis are rooted in tar production. This is likely due to hydrogen from biomass that disrupts the crosslinking of fragmented aromatic structures during coal pyrolysis to produce tar rather than char. This is consistent with Solomon's description of coal pyrolysis, where hydrogenated aromatic structures of low molecular weight are likely to be

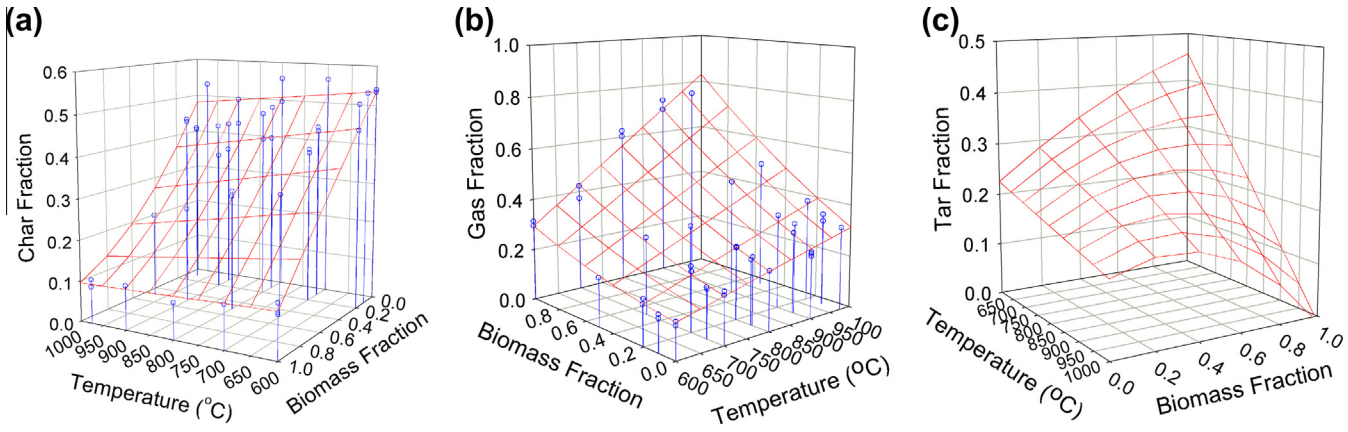

Fig. 3. (a) Char, (b) gas, and (c) tar product distributions for PRB/WB co-pyrolysis.

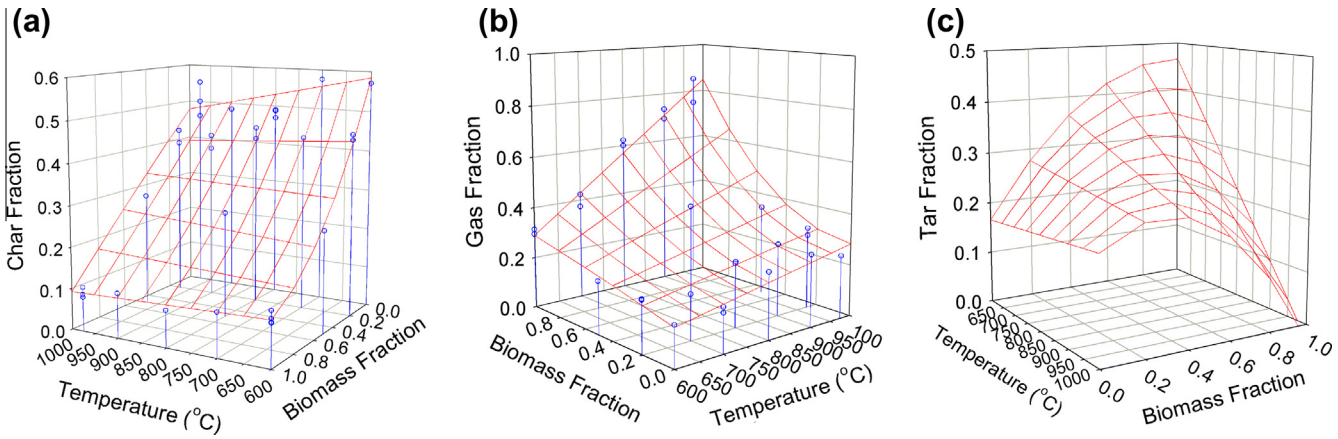

Fig. 4. (a) Char, (b) gas, and (c) tar product distributions for LIG/WB co-pyrolysis.

released as tar, provided that they escape before crosslinking reactions can occur [23].

As discussed above, Haykiri-Acma and Yaman note that lower rank coals yield more synergies in co-pyrolysis with biomass, although they attribute this behavior to overlapping regions of high mass loss at lower temperatures for low rank coals in their TGA-based experiments, while higher rank coals pyrolyze at higher temperatures relative to biomass [11]. For the high heating rates and low gas residence times used in the current study, Figs. 3c and 4c show that synergies in coal/biomass co-pyrolysis increase with decreasing coal rank from sub-bituminous (B) to lignite at high temperatures. Under similar conditions with bituminous coals, additive (non-synergistic) behavior was observed in a few studies [8,16,34], while some synergy was observed in other studies [17–19]. These results are complicated by the use of herbaceous biomass in several of these studies [17–19,34], which typically contains higher concentrations of alkali and alkaline earth metals in its ash, and may be capable of catalyzing pyrolysis reactions to some extent. In general, however, evidence from the literature does point to increased co-pyrolysis synergy for lower rank coals, which is supported by this work. This is likely due to the lower initial aromatic content of the lower ranked coals [18,22], which may affect synergy through either increased quantities of low-molecular weight primary pyrolysis fragments available for hydrogen

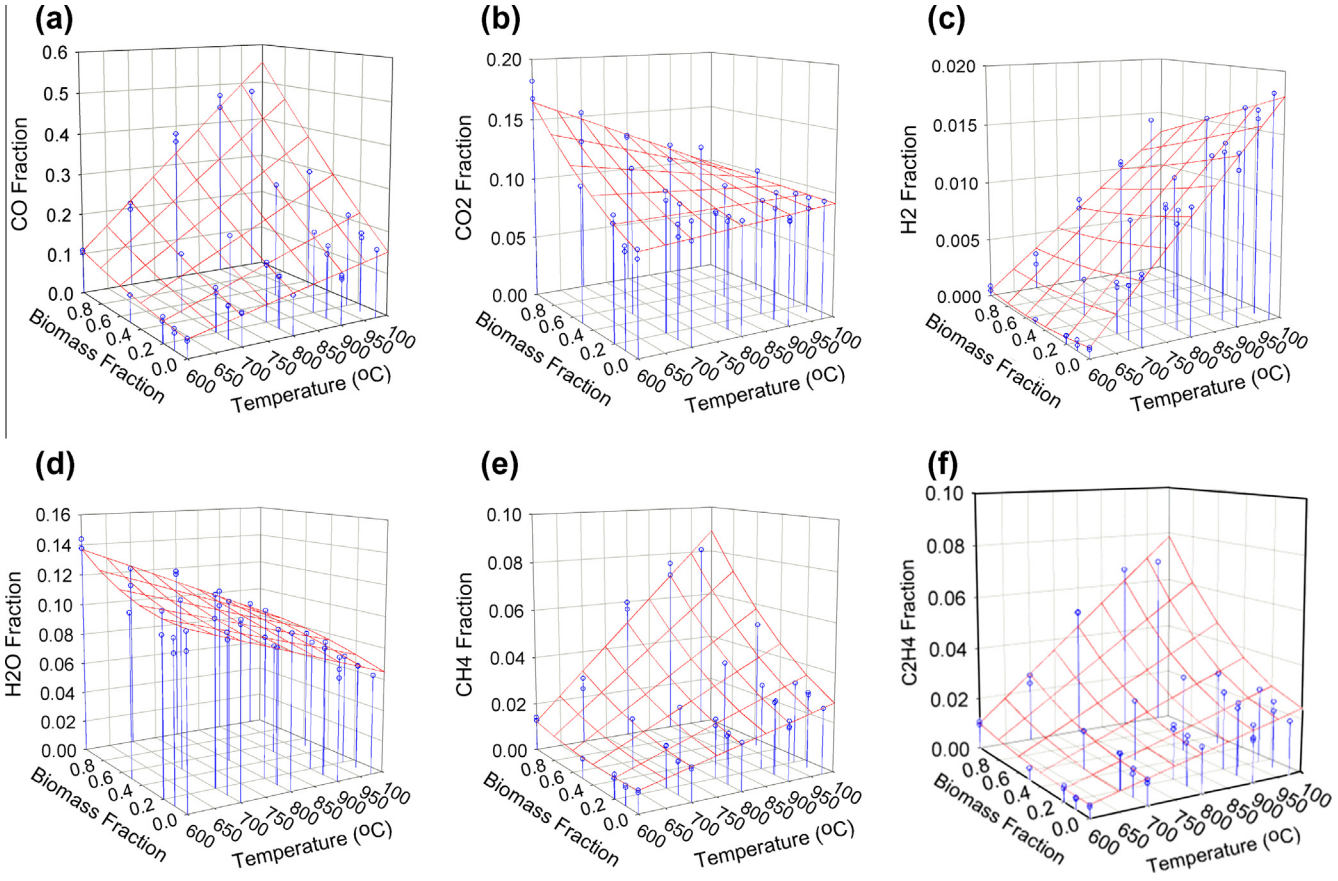

Fig. 5. PRB/WB gas species distributions and curve fits for (a) CO, (b) CO_2, (c) H_2, (d) H_2O, (e) CH_4, and (f) C_2H_4.

acceptance [23], or through higher macro- and meso-pore volumes [22] which facilitate penetration of biomass volatiles during reaction.

3.2. Major species product distributions

Quantitative gas measurements for CO, CO_2, H_2, H_2O, CH_4, and C_2H_4 are taken for each test. Distributions of gaseous products for PRB/WB and LIG/WB are shown in Figs. 5 and 6, respectively. It can be seen that CO, H_2, CH_4, and C_2H_4 gas species exhibit increased production with temperature, and H_2O and CO_2 yields generally decrease with temperature, though CO_2 appears to increase slightly with temperature for pure PRB coal pyrolysis.

Similar trends in CO_2 production with temperature and feedstock are seen in other studies [17–20], while lack of explicitly conveyed water evolution prevents quantitative comparison of the water data. In biomass, CO_2 and H_2O production trends can be attributed to release of oxygenated gases from cellulose and hemicellulose decomposition at low temperatures, with preferential volatile decomposition to CO and CH_4 at higher temperatures [20]. For low rank coals with more than 10% oxygen content, as are used here, CO_2 and H_2O release at low temperature is related to low temperature crosslinking, which is replaced by other processes at high temperature [14,23]. As a result, there appears to be relatively little temperature dependence on CO_2 and H_2O evolution for either coal species, as these primarily occur at temperatures lower than the minimum temperature of 600 °C here. Likewise, as the energy barrier for these reactions is fairly low, there is little nonlinearity in CO_2 and H_2O production as a function of biomass fraction. What little nonlinearity exists may occur when cross-linking in oxygenated functional groups from low-rank coals (associated with low temperature pyrolysis for low heating rates) is increasingly disrupted at higher temperatures due to increasing amounts of available hydrogen from biomass, yielding lower CO_2 and H_2O production with increased temperature.

The primary nonlinearities in gas production are due to reductions in hydrocarbon species CH_4 and C_2H_4 upon co-pyrolysis, with additional nonlinearities from CO at high temperature in the LIB/WB blends, and H_2 at all temperatures for this blend. During pyrolysis of coal, release of methane and other light aliphatic species is associated with crosslinking, or recombination, reactions in which clusters of aromatic structures combine to create more stable secondary char structures [23]. As noted above, hydrogen readily bonds to the active sites on these aromatic clusters to produce tars before these crosslinking reactions can occur. The net effect upon co-pyrolysis is a synergistic reduction in CH_4, C_2H_4, and H_2 species, with an increase in tar production, as seen in Figs. 3–6. It has been noted in other studies that aliphatic species may play a significant role in producing synergies in co-pyrolysis [12,35], thus H_2 gas from biomass pyrolysis may not be the only hydrogen donor in preventing crosslinking, and may instead be abstracted from the aliphatic molecules themselves [23].

Inspection of the hydrogen content of all gas species shows that atomic hydrogen does increase with biomass wt%. By tracking atomic gas phase hydrogen, as seen in Fig. 7, it can be seen that methane, ethylene, and other light hydrocarbons are the favored destinations for hydrogen in biomass. The favored formation of such products over H_2 supports the theory that coal radicals are stabilized by H_2 donated from biomass, which may be consumed in those reactions. One other trend to note from Fig. 7 is the large bias of PRB coal to produce H_2 rather than hydrocarbons, however, inspection of the time-dependent release of gas species from the

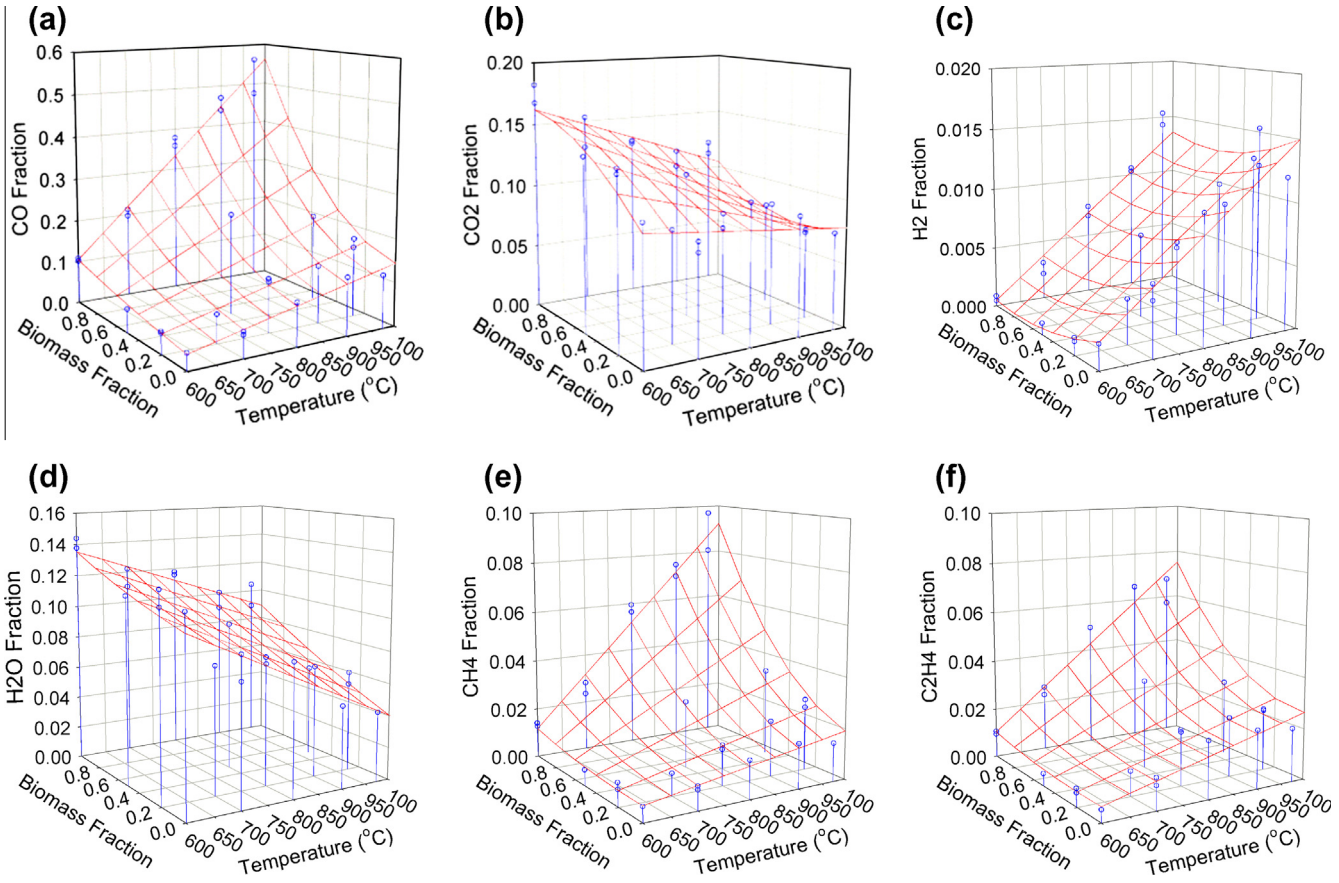

Fig. 6. LIG/WB gas species distributions and curve fits for (a) CO, (b) CO_2, (c) H_2, (d) H_2O, (e) CH_4, and (f) C_2H_4.

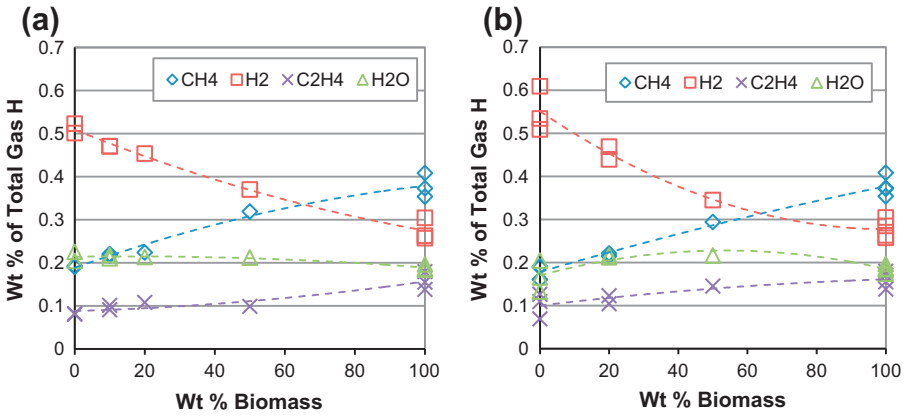

Fig. 7. Atomic hydrogen tracking for (a) PRB and (b) LIG at 975 °C.

feedstocks on pyrolysis reveals that hydrogen in coal is evolved very slowly relative to biomass, and is the result of the condensation of aromatic ring structures for prolonged heat treatment times as are used in this work [23].

This is illustrated in Fig. 8, where 90% of the H_2 from biomass is evolved within the first 10 s, while significant quantities of H_2 are evolving from PRB coal and the PRB/WB blends a minute into the pyrolysis reaction, due to ring condensation processes. Calculated H_2 release from the 80/20 and 50/50 blends, based on additive behavior, are also plotted in Fig. 8, predicting higher total release of H_2 than those measured for these blends. The rate of H_2 evolution from the PRB/WB blends in the later stages of pyrolysis are consistent with that of ring condensation processes in the coal char from these blends, though the initial production of H_2 is lower, which accounts in essence for the total difference of the data from the calculated additive production history. This deficiency in initial H_2 production also suggests that it is consumed early in the co-pyrolysis reaction, likely in stabilizing tar radicals as suggested above. Similar H_2 production trends also appear for fuel blends at the other temperatures studied.

To further validate the hypothesis that hydrogen from biomass pyrolysis stabilizes coal tar radicals, a few additional PRB coal pyrolysis tests were performed in which 10% hydrogen gas (by volume) was added to the argon sweep gas. The major product distribution results are shown in Fig. 9, along with curve fits from Eq. (1) for PRB coal pyrolysis in an inert argon sweep gas. The primary effect of the presence of hydrogen is a large increase in tar production and a corresponding decrease in char production, while gas and water evolution are fairly insensitive to the presence of hydrogen. Thus hydrogen is shown to favor production of tar, rather than secondary char, from radicals formed early in the coal pyrolysis process, similar to the early studies of hydropyrolysis for the production of coal tar liquids [36,37].

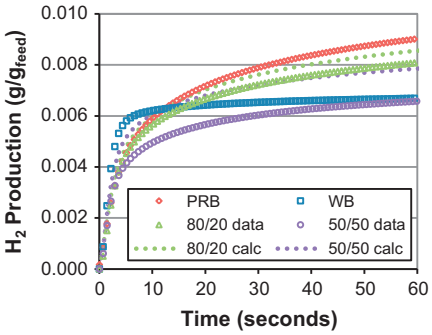

Fig. 8. Gaseous H_2 evolution for pyrolysis at 800 °C.

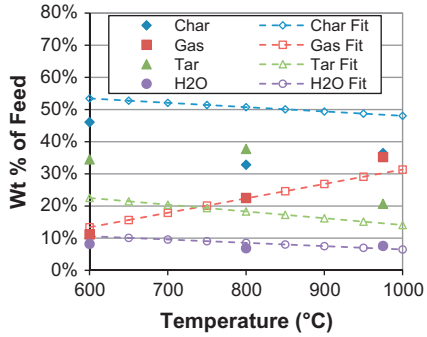

Fig. 9. Major product distributions for PRB coal pyrolysis with 10% hydrogen by volume in the argon background gas. Fit lines are from Eq. (1) for the case with no hydrogen.

3.3. Minor species product distributions

Gas bags samples for 800 °C experiments were collected and analyzed by GC–MS. The resulting chromatogram is shown in Fig. 10. It can be seen that gaseous cyclic and acyclic C_2—C_5 hydrocarbon species are released from all feeds while oxygenated hydrocarbons such as acetaldehyde (C_2H_4O) appear to be exclusive to biomass. Sulfurous compounds such as carbonyl sulfide (COS) and hydrogen sulfide (H_2S) are exclusive to coal. This is also expected as biomass contains a negligible amount to sulfur as seen from Table 2.

Also notable in Fig. 10 is the apparent abundance of light aromatics, i.e. benzene (C_6H_6) and toluene ($C_6H_5CH_3$), found in the biomass gas, compared to that found in PRB or LIG gas. Further, adding just 20% biomass to PRB coal appears to significantly increase the benzene and toluene content in the resulting gas, supporting the hypothesis that rapid evolution of atomic hydrogen from the biomass contributes to hydropyrolysis of coal and the enhanced production of light aromatic tars that yields the co-pyrolysis nonlinearity [23,25]. This result does differ from that of Jones et al., who note that aliphatic species are almost completely absent from their co-pyrolysis tars; however, this may be due to the high tar residence times inherent in their experiments, where aliphatic tar species have had ample time to crack into gases and secondary char [12].

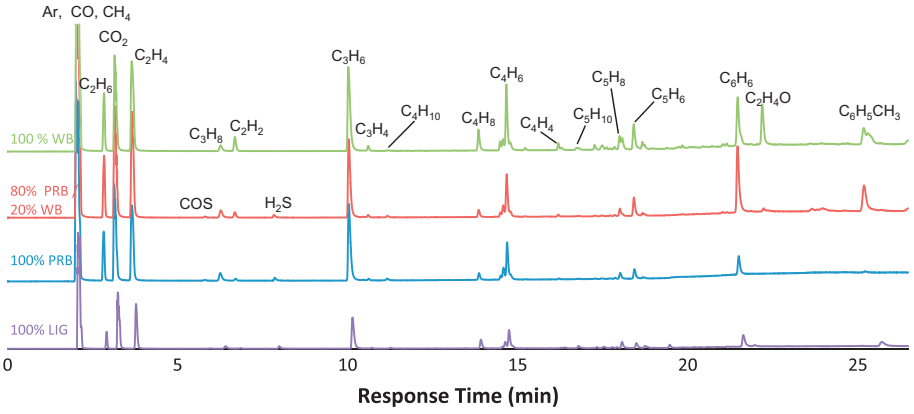

Fig. 10. Chromatogram of minor gas constituents collected at 800 °C.

Table 3
PRB/WB product distribution coefficients for Eq. (1).

i	a_0	a_X	a_{XX}	a_T	a_{XT}	a_{XXT}	R^2
Char	6.153E−1	−8.006E−2	−3.989E−1	−1.348E−4	−5.304E−4	6.241E−4	0.945
CO_2	5.646E−2	1.297E−1	7.911E−2	3.523E−5	−1.242E−4	−7.901E−5	0.882
CO	−1.215E−1	−4.381E−1	−2.976E−3	2.733E−4	7.845E−4	5.781E−5	0.981
CH_4	−2.051E−2	−5.942E−2	−2.356E−2	4.843E−5	9.252E−5	5.181E−5	0.973
C_2H_4	−2.456E−2	−2.325E−2	−4.506E−2	4.856E−5	3.753E−5	8.522E−5	0.958
H_2	−2.489E−2	2.488E−3	3.844E−3	4.289E−5	−7.475E−6	−3.697E−6	0.983
H_2O	1.681E−1	−4.893E−2	9.816E−2	−1.031E−4	8.166E−5	−1.122E−4	0.802
Tar	3.516E−1	5.175E−1	2.894E−1	−2.105E−4	−3.342E−4	−6.240E−4	0.743

Table 4
LIG/WB product distribution coefficients for Eq. (1).

i	a_0	a_X	a_{XX}	a_T	a_{XT}	a_{XXT}	R^2
Char	7.429E−1	−1.459E+0	8.515E−1	−2.646E−4	1.095E−3	−8.734E−4	0.977
CO_2	1.226E−1	3.678E−1	−2.421E−1	−4.412E−5	−4.195E−4	3.196E−4	0.844
CO	−1.297E−1	4.325E−2	−4.951E−1	2.743E−4	1.443E−5	8.555E−4	0.972
CH_4	−1.313E−2	−2.979E−2	−6.625E−2	3.214E−5	4.889E−5	1.204E−4	0.977
C_2H_4	−2.483E−2	−2.205E−3	−5.973E−2	5.117E−5	7.679E−7	1.099E−4	0.930
H_2	−1.726E−2	−9.410E−4	−9.411E−4	3.224E−5	−6.300E−6	6.751E−6	0.942
H_2O	2.021E−1	−4.135E−3	6.766E−3	−1.616E−4	4.243E−5	3.323E−6	0.907
Tar	1.183E−1	1.085E+0	5.845E−3	8.049E−5	−7.755E−4	−5.420E−4	0.868

3.4. Multi-parameter fitting

In Figs. 3–6, it is evident that product distributions are fairly linear with respect to temperature, and may be nonlinear with respect to biomass fraction, leading to the form of the curve-fit equation in Eq. (1). The coefficients for each product, i, are given in Tables 3 and 4 for PRB/WB and LIG/WB mixtures, respectively, and are applicable over: $0 < X < 1$ and $600 < T\,(°C) < 975$. The curve fits represented by these coefficients are shown as the red[1] meshes in the above figures. Char fractions given by this equation are simply the remaining solid fraction after pyrolysis, and include both fixed carbon and ash constituents.

Fits of the data to Eq. (1) are shown to be fairly good, with R^2 correlation values of 0.8 and higher, as listed in Tables 3 and 4. Water vapor and CO_2 both consistently yield lower R^2 correlation values, though this may be attributed to the relatively higher mean values and lower variability of these species across the input parameter space, relative to the "better-correlated" species. The correlation of the tar curve fit to its available data points is also low, as it is computed by difference from the curve fits of the other seven species to enforce mass conservation, rather than being fit to the tar production data points, which have higher inherent uncertainty.

4. Conclusions

Co-pyrolysis of southern yellow pine with a sub-bituminous Powder River Basin coal and Mississippi lignite at several temperatures and feed ratios have been shown in this study to yield significant nonlinearities, particularly at higher temperatures and for decreasing coal rank. The data from this study suggests that rapid pyrolysis of biomass produces hydrogen that stabilizes large radical structures generated during the early stages of coal pyrolysis. Stabilization causes these structures to be released as tar, rather than crosslinking with one another to produce secondary char and light gases. For this to occur, coal and biomass particles must undergo rapid heating during co-pyrolysis, and the particles should be in close proximity to one another so that the fresh biomass volatiles can interact with the pyrolyzing coal particles. The current study shows that the evolution of atomic hydrogen from biomass can take either the form of H_2, CH_4, or other hydrocarbons,

[1] For interpretation of color in Fig. 3, the reader is referred to the web version of this article.

which may be used to stabilize the aromatic coal pyrolysis radicals. In addition, the rapid evolution and quenching inherent in these experiments shows that tar is the primary synergistic product of co-pyrolysis. This was verified in coal pyrolysis experiments in a hydrogen environment, which produced more tar and less char than those in an inert environment, with gas production being largely unaffected. Some studies show that additional gas is the primary product of co-pyrolysis, however, these studies have moderate to long tar residence times which promotes cracking of the co-pyrolysis tars to light gases. Finally, it is shown that, for the two coal types tested, co-pyrolysis synergies are more significant as coal rank decreases, likely because the initial coal structures contain increasingly larger pores and smaller clusters of aromatic structures, which are more readily retained as tar in rapid co-pyrolysis.

Although the data in this study provides a reasonably sound basis for proving that hydrogen donation from biomass promotes non-additive tar production on rapid co-pyrolysis with low rank coals, additional studies could provide further proof of this mechanism. In particular, analysis of heavier tar compounds from co-pyrolysis would shed some light on whether the synergistic portion of the tar production does in fact originate with the coal feedstock. Likewise, a detailed analysis of the resulting char structures may indicate whether secondary char formation is reduced in co-pyrolysis, as suggested by this study's data. Finally, increasing pyrolysis pressures, increasing particle sizes, or decreasing sweep gas flow rates may give a sense for the effect of tar cracking on the overall co-pyrolysis product distributions, and suggest kinetic rates for these reactions.

Acknowledgements

The authors wish to thank Monica Nicola for assistance with the data analysis. Inquiries about the C3M software can be directed to Dirk VanEssendelft at dirk.vanessendelft@netl.doe.gov.

This technical effort was performed under the RES contract DE-FE0004000, as part of the National Energy Technology Laboratory's Regional University Alliance (NETL-RUA), a collaborative initiative of the NETL. This project was funded by the Department of Energy, National Energy Technology Laboratory, an agency of the United States Government, through a support contract with URS Energy & Construction, Inc. Neither the United States Government nor any agency thereof, nor any of their employees, nor URS Energy & Construction, Inc., nor any of their employees, makes any warranty, expressed or implied, or assumes any legal liability or responsibility for the accuracy, completeness, or usefulness of any information, apparatus, product, or process disclosed, or represents that its use would not infringe privately owned rights. Reference herein to any specific commercial product, process, or service by trade name, trademark, manufacturer, or otherwise, does not necessarily constitute or imply its endorsement, recommendation, or favoring by the United States Government or any agency thereof. The views and opinions of authors expressed herein do not necessarily state or reflect those of the United States Government or any agency thereof.

References

[1] Ruppert LF et al. The US Geological Survey's national coal resource assessment: the results. Int J Coal Geology 2002;50:247–74.
[2] Young P. Quarterly coal report. March 2012. U.S. Energy Information Administration.
[3] Kiehl JT et al. Earth's annual global mean energy budget. Bull Am Meteorol Soc 1997;78:197–208.
[4] McKendry P. Energy production from biomass (part 1): overview of biomass. Bioresour Technol 2002;83:37–46.
[5] Wihersaari M. Evaluation of greenhouse gas emission risks from storage of wood residue. Biomass Bioenergy 2005;28:444–53.
[6] Kirubakaran V et al. A review on gasification of biomass. Renew Sust Energy Rev 2009;13:179–86.
[7] Werther J et al. Combustion of agricultural residues. Progr Energy Combust Sci 2000;26:1–27.
[8] Moghataderi B et al. Pyrolytic characteristics of blended coal and wood biomass. Fuel 2004;83:745–50.
[9] Higman C. Gasification. Boston: Elsevier/Gulf Professional Pub; 2003.
[10] Chen WH, Wu JS. An evaluation of rice husks and pulverized coal blends using a drop tube furnace and a thermogravimetric analyzer for application to a blast furnace. Energy 2009;34:1458–66.
[11] Haykiri-Acma H, Yaman S. Interaction between biomass and different rank coals during co-pyrolysis. Renew Energy 2010;35:288–92.
[12] Jones JM, Kubacki M, Kubica K, Ross AB, Williams A. Devolatilisation characteristics of biomass and coal blends. J Anal Appl Pyrolysis 2005;74:502–11.
[13] Pan YG, Velo E, Puigjaner J. Pyrolysis of blends of biomass with poor coals. Fuel 1996;75:412–8.
[14] Sonobe T et al. Synergies in co-pyrolysis of Thai lignite and corncob. Fuel Process Technol 2008;89:1371–8.
[15] Vuluthuru HB. Investigations into the pyrolytic behaviour of coal/biomass blends using thermogravimetric analysis. Bioresour Technol 2004;92:187–95.
[16] Meesri C et al. Lack of synergetic effects in the pyrolytic characteristics of woody biomass/coal blends under low and high heating rate regimes. Biomass Bioenergy 2012;23:55–66.
[17] Zhang L et al. Co-pyrolysis of biomass and coal in a free fall reactor. Fuel 2007;86:353–9.
[18] Wei L et al. Effects of feedstock on co-pyrolysis of biomass and coal in a free-fall reactor. J Fuel Chem Technol 2011;39(10):728–34.
[19] Yuan S et al. Rapid co-pyrolysis of rice straw and bituminous coal in a high-frequency furnace and gasification of the residual char. Bioresour Technol 2012;109:188–97.
[20] Park DK et al. Co-pyrolysis characteristics of sawdust and coal blend in TGA and a fixed bed reactor. Bioresour Technol 2010;101:6151–6.
[21] Seo MW, Kim SD, et al. Pyrolysis characteristics of coal and RDF blends in non-isothermal and isothermal conditions. J Anal Appl Pyrolysis 2010;88(2):160–7.
[22] Laurendeau NM. Heterogeneous kinetics of coal char gasification and combustion. Progr Energy Combust Sci 1978;4:221–70.
[23] Solomon PR, Serio MA, Suuberg EM. Coal pyrolysis: experiments, kinetic rates and mechanisms. Progr Energy Combust Sci 1992;18:133–220.
[24] Saxena SC. Devolatilization and combustion characteristics of coal particles. Progr Energy Combust Sci 1990;16:55–94.
[25] Anthony DB, Howard JB. Coal devolatilization and hydrogasification. AIChE J 1976;22:625–56.
[26] Sjöström K et al. Promoted reactivity of char in co-gasification of biomass and coal: synergies in the thermochemical process. Fuel 1999;78:1189–94.
[27] Nelson JM et al., Low-rank coal gasification studies using the PSDF transport gasifier. In: Western fuels symposium: 20th international conference on lignite, brown, and subbituminous coal, Denver, CO; 2006.
[28] Southern Company Services, Inc. Power systems development facility – final report, DOE Cooperative Agreement: DE-FC21-90MC25140; 2009.
[29] Breault RW, Guenther C. Mass transfer coefficient prediction method for CFD modeling of riser reactors. Powder Technol 2010;203:33–9.
[30] Guenther C, Shahnam M, Syamlal M et al. CFD Modeling of a Transport Gasifier. In: 19th International Pittsburgh coal conference. Pittsburgh, PA; 2002.
[31] Guenther C, Syamlal M, Longanbach J, Smith PV. CFD Modeling of a Transport Gasifier Part II. In: 20th International Pittsburgh coal conference. Pittsburgh, PA; 2003.
[32] Guenther C, VanEssendelft DT, Chaundhari K, et al. Gasification modeling in the 21st century. Power Eng 2012;116:80–2.
[34] Weiland NT et al. Product distributions from isothermal co-pyrolysis of coal and biomass. Fuel 2012;94:563–70.
[35] Suelves I, Lazaro MJ, Moliner R. Synergetic effects in the co-pyrolysis of samca coal and a model aliphatic compound studied by analytical pyrolysis. J Anal Appl Pyrolysis 2002;65:197–206.
[36] Fynes G, Ladner WR, Newman JOH. The hydropyrolysis of coal to BTX. Progr Energy Combust Sci 1980;6:223–32.
[37] Zhu Z, Ma Z, Zhang C, Jin H, Wang X. Flash hydropyrolysis of northern Chinese coal. Fuel 1996;75:1429–33.